atmosphere

MDPI

Article

Model-Based Evaluation of Dew Condensation Potential Across Contrasting Climates Using Field Observations, ERA5, CORDEX, and Local Weather Data

Soroush Moradi Zavie Kord [1,*], Szabolcs Galambosi [1], Juhana Hirvilahti [1], Nahid Atashi [2], Tareq Hussein [2,3], Laura Alakukku [1], Petri Pellikka [4,5,6] and Juuso Tuure [1]

[1] Department of Agricultural Sciences, University of Helsinki, Koetilantie 5, P.O. Box 28, FI-00014 Helsinki, Finland
[2] Institute for Atmospheric and Earth System Research (INAR/Physics), Faculty of Science, University of Helsinki, FI-00014 Helsinki, Finland
[3] Environmental and Atmospheric Research Laboratory (EARL), Department of Physics, School of Science, University of Jordan, Amman 11942, Jordan
[4] Department of Geosciences and Geography, University of Helsinki, P.O. Box 64, FI-00014 Helsinki, Finland
[5] Finnish Southern Africa Cooperation Institute, 10 Schwabe Street, Windhoek 10005, Namibia
[6] State Key Laboratory for Information Engineering in Surveying, Mapping and Remote Sensing, Wuhan University, Wuhan 430072, China
* Correspondence: soroush.moradizaviekord@helsinki.fi

Abstract

Dew condensation on passive collectors can supplement water availability across different climates, but its prediction remains uncertain because condensation depends on both atmospheric conditions and collector properties. This study evaluated a physically based model of dew condensation potential (horizontal condenser surface) using field observations from four sites: Helsinki (Finland), Maktau (Kenya), Ajaccio (Corsica, France), and Bordeaux (France). Simulations were primarily driven by ERA5 reanalysis data, while on-site weather station data were used for sensitivity analysis where available. Near-future dew behavior at the European sites was further examined using EURO-CORDEX climate data. The model reproduced the general timing and cumulative progression of condensation, but predicted yields were generally greater than observed yields, especially at Helsinki and Maktau. The best agreement was obtained by Bordeaux, where the experimental setup closely matched the model assumptions. On-site weather stations data improved agreement, highlighting the importance of site-specific nocturnal conditions. CORDEX simulations showed clear site differences, with Bordeaux having the highest and most stable projected condensation potential, Ajaccio frequent but low-intensity condensation, and Helsinki lower annual totals but comparable yield per dew night. The results show that the model was useful for comparing relative condensation potential across climates and identifying dew seasons, but accurately estimating the harvestable dew requires better representation of collector properties such as geometry and surface.

Keywords: atmospheric water harvesting; dew modelling; radiative cooling; water scarcity

Check for updates

Academic Editors: Daniel Beysens and Marc Muselli

Received: 15 May 2026
Revised: 22 June 2026
Accepted: 24 June 2026
Published: 29 June 2026

Copyright: © 2026 by the authors. Licensee MDPI, Basel, Switzerland. This article is an open access article distributed under the terms and conditions of the Creative Commons Attribution (CC BY) license.

1. Introduction

Freshwater scarcity is a growing problem as our climate and landscapes continue to change [1]. This issue is especially serious in places with scarce and sporadic rainfall. In these areas, alternative sources of water [2] like dew and fog can play an important role.

In water-scarce areas, dew formation, unlike precipitation, may be available for collection year-round through nocturnal radiative cooling and local atmospheric conditions, making it a passive source of water that does not rely on secondary energy infrastructure and resources. Field studies across a wide range of climates have demonstrated that dew formation may occur frequently, from cold temperate climates of northern environments to semi-arid [3–5] Mediterranean coastal and oceanic temperate regions [3–11]. The availability of dew in broad climatic regions highlights the relevance of dew as a non-rainfall water input in different atmospheric settings, especially in drought-prone water-scarce areas.

Passive dew collectors are surfaces designed to promote dew collection and enable its collection. Generally, passive dew collectors for which results have been reported are insulated 1 m^2 low-density polyethylene surfaces tilted to 30° with respect to the horizon [3–5,7,9,12,13]. These types of collectors are considered standard dew collectors (Standard collector). Recorded mean nightly yields of passive dew collectors are often low, ranging from 0.069–0.145 mm/night [3,5,6,12,14–18] while the maximum recorded value in field conditions is 0.6 mm/night [9], and the theoretical maximum yield is 0.7–0.8 mm/night. Despite the small daily yields, cumulative yields over time can make dew a meaningful supplementary water source [4,17–19], especially with dew collector enhancements in forms of geometry and material properties [3,4,20,21].

Dew condensation occurs at night when an exposed surface cools below the dew point of the surrounding air, resulting in condensation due to an imbalance between radiative losses and convective and latent heat. The process is dominated by the physical properties of the condensing surface and meteorological variables, including air temperature, air relative humidity, wind speed, cloud cover, and longwave radiation [7].

Because condensation happens within a thin atmospheric boundary layer close to the surface, surface-atmosphere energy exchange plays an important role in determining both the occurrence and final dew yield on the condenser film. Experimental work has shown that surface emissivity, thermal insulation, geometry, and drainage efficiency can affect or enhance the dew yields, sometimes by factors comparable to or exceeding those associated with meteorological variability alone [3,7,21,22]. These findings highlight that dew formation is not only an atmospheric phenomenon but a process resulting from surface and atmospheric dynamics.

To estimate dew formation beyond field experiments, a range of modelling approaches has been developed. Most dew models are based on surface energy balance, in which radiative cooling is balanced by convective heat transfer, conductive fluxes, and the latent heat released during condensation [8,12,15,21,23–26]. Such models have been applied to specific sites as well as regional and global assessments, often using reanalysis datasets (e.g., ERA5) to provide the meteorological conditions required to run the model simulations.

While condensation models differ in complexity and necessary parameters, comparisons and validation studies indicated that physically based dew models can reproduce measured yields within an uncertainty range of approximately 30–40% [8,26,27]. Such agreement level shows that the unavoidable simplifications in condenser surface and uncertainties in near-surface meteorological inputs, especially when coarse resolution reanalysis data such as global datasets are employed. Moreover, this uncertainty range is widely accepted in the literature [3,8,26,27] as representative of the natural variability of dew formation rather than a shortcoming of any single modelling framework.

Among existing approaches, surface energy balance models along with reanalysis data have proven useful for exploring the spatial and temporal variability of dew formation. A notable example is the model developed by Vuollekoski et al. [28], which simulates dew formation on an artificial condensing surface using the heat and mass balance equations driven by meteorological inputs. The model is open source and could be run using re-

analysis datasets such as ERA-Interim and ERA-5 provided by the European Centre for Medium-Range Weather Forecasts (ECMWF).

Previous studies have adopted this model and evaluated the potential of dew collection in different climates [27,29,30]. However, they have also highlighted the importance of assessing the model performance against long-term field observations before applying and concluding the results to regional mapping; this point has been highlighted due to the uncertainty of the model and, of course, the uncertainty of reevaluated data such as ERA5.

Despite this progress, two important gaps remain: First, most existing evaluations of dew models' performance are limited either to a single climatic region or to broad-scale applications that do not sufficiently assess site-level behavior, making it difficult to evaluate model robustness across contrasting atmospheric conditions. Second, while reanalysis data such as ERA-Interim have been used in previous studies to run the dew model [27,31], the use of climate models to study near-future dew behavior inform of forecasts and seasonal shifts has remained limited.

Availability of multiple experimental dew collections in different climatic regions throughout the past two decades makes it possible to re-examine the model measurements. In addition to conventional standard dew collectors, new field experiments containing active surface management, such as automatic wiping of condensing surfaces [4] and sandblasting the condenser surface [3], have also demonstrated that an unconventional approach to increase the yield through multiple automatic wiping or increasing the nucleation sites through an increase of surface roughness can significantly influence measured dew yields without changes in atmospheric parameters.

These findings suggest that differences between modelled and observed dew yields may come not only from meteorological uncertainty but also from other factors, including surface processes/properties that are simplified or excluded in most models. Recognizing and quantifying these limitations is essential when interpreting model performance and when extending model results toward practical applications.

This study aimed to evaluate how well a physically based dew condensation model performs in contrasting climatic conditions and to examine whether the same model can be used for near-future dew forecasting. The study aims to strengthen the use of dew models for site evaluation, climatic comparison, and atmospheric water resource assessment.

2. Materials and Methods

This study evaluated the performance of a dew formation model under different climatic conditions using field observations and multiple meteorological datasets. The measured dew yield data from four geographically distinct sites were also included; Helsinki (Finland), Maktau (Kenya), Ajaccio (Corsica, France), and Bordeaux (France), these were used to assess model performance across humid continental climate Dwa, hot semiarid climate Bsh, oceanic climate Cfb, and hot-summer Mediterranean climate Csa environments (Figure 1).

Simulations were primarily conducted using the ERA5 reanalysis dataset [31], while on-site weather station data were additionally used for comparison. Regional climate projection data from the EURO-CORDEX [31–33] were further applied to examine the potential of future changes in dew formation under projected climatic regions and conditions with consideration of climate change.

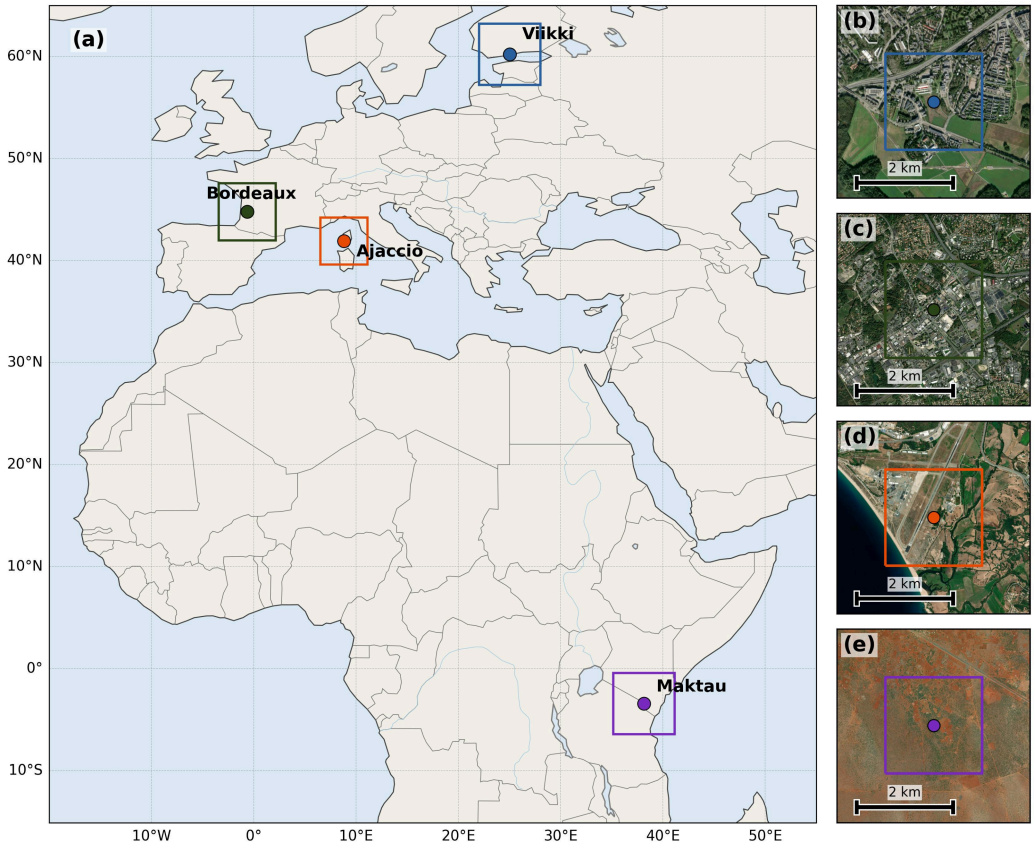


Figure 1. Study sites used for dew modelling and evaluation: (**a**) overview map showing all locations; (**b**) Helsinki, Viikki, Finland (60.23° N, 25.05° E); (**c**) Bordeaux, France (44.84° N, 0.58° W); (**d**) Ajaccio, Corsica, France (41.92° N, 8.74° E); (**e**) Maktau (3.43° S, 38.14° E).

2.1. Dew Formation Model

Dew formation was simulated using a physically based surface energy balance model developed by Vuollekoski et al. and later applied in regional studies by Atashi et al. The model follows a surface energy balance and builds upon earlier analytical and experimental dew models (e.g., [16,22]). The model describes condensation on an artificial, horizontal condenser surface with a fixed area of 1 m^2 that is thermally insulated from the ground heat flux. Dew formation is simulated by solving heat and mass balance equations at sub-daily temporal resolution using near-surface meteorological parameters (full formulation is presented in Appendix A.1).

It is worth mentioning that a sensitivity test for collector inclination was not performed in this study. The dew formation model used here represents condensation on a horizontally thermally insulated surface and does not include collector tilt as a parameter. Therefore, representing a 30° field collector would require structural modification of the model formulation, including changes in radiative exchange, convective heat transfer, and drainage assumptions. For this reason, the present study applied the original model configuration and evaluated its performance against field observations with different collector setups.

The temporal evolution of the condenser temperature T_c is governed by the heat balance equation:

$$\frac{dT_c}{dt}(C_c m_c + C_w m_w + C_i m_i) = P_{\text{rad}} + P_{\text{cond}} + P_{\text{conv}} + P_{\text{lat}} \quad (1)$$

where C_c, C_w, and C_i are the specific heat capacities of the condenser material, liquid water, and ice, respectively, and m_c, m_w, and m_i are their corresponding masses. The terms on the

right-hand side represent radiative (P_{rad}), conductive (P_{cond}), convective (P_{conv}), and latent (P_{lat}) heat exchange.

The condensation rate is calculated from the vapor pressure gradient between the air and the condenser surface:

$$\frac{dm}{dt} = \max(0, S_c k[p_{sat}(T_d) - p_{sat}(T_c)]), \quad (2)$$

where S_c is the condenser surface area, k is the mass transfer coefficient, T_d is the dew point temperature, p_{sat} indicates saturation vapor pressure, and m represents the mass of condensed water or ice depending on surface temperature. Convective heat transfer was parameterized as a function of wind speed at 2 m height following Richards et al. [25], and phase changes between liquid water and ice were handled according to the formulation of Vuollekoski et al. [28].

The mass transfer coefficient k was not a fixed value but calculated dynamically at each model time step from the convective heat transfer coefficient and atmospheric pressure. To assess sensitivity to this parameterization, additional simulations were carried out (Figure A1 in Appendix B) using several published formulations for heat transfer (available at Vuollekoski et al., 2015 [28]). These tests showed that the cumulative dew curves retained similar seasonal structure across parameterizations, while the total accumulated dew varied in magnitude. This suggests that the choice of k-related parameterization mainly influences the simulated amount of condensation rather than the occurrence of condensation periods.

The Vuollekoski et al., 2015 [28] model integrates Equations (1) and (2) over time and tracks the cumulative mass of condensed water and ice. Daily dew yield was defined as the maximum accumulated condensation within a diurnal cycle. In the model output, a day with simulated condensation was defined as any diurnal cycle with positive simulated condensate accumulation. This represented a condensation potential on the modelled surface and was therefore not directly equivalent to a field-observed dew day. In addition, the evaporation of condensed water during daytime was not considered, assuming that dew was collected shortly after sunrise.

Fog deposition, precipitation, and non-condensational surface wetting were not explicitly simulated. These assumptions are consistent with previous models [27,28] and allow comparison across different climatic regions. The full model formulation, including the expressions for radiative, convective, and latent heat terms, is provided in Appendix A (Appendices A.1 and A.2).

2.2. Field Observations and Study Sites

Field observations of dew condensation from four locations were used to evaluate the modelled dew formation under different climatic conditions (Figure 1). The selected sites include northern temperate, semi-arid tropical, Mediterranean coastal, and oceanic temperate environments, bringing a broad range of atmospheric conditions relevant for dew formation. Site locations included Helsinki (Finland), Maktau (Kenya), Ajaccio (Corsica, France), and Bordeaux (France).

The Helsinki site (60.23° N, 25.05° E) located on the Viikki campus of the University of Helsinki, Finland. It represents a cool northern temperate climate with strong seasonal variation in radiation and temperature, with the dew season starting in May until end of September. Two experimental campaigns were conducted at this site: from 17 June to 31 August 2022 and from 7 July to 30 September 2024. Dew was measured using a standard 1 m^2 passive dew collector with three polyvinyl chloride (PVC) condenser surfaces, installed at a 30° inclination angle with an insulated back, matching the standard condenser geometry used in previous dew studies [3–6,12,14–16] (Figure 2). Details of the 2022 and 2024 campaign and collector performance are reported by Kord et al. [3,4].

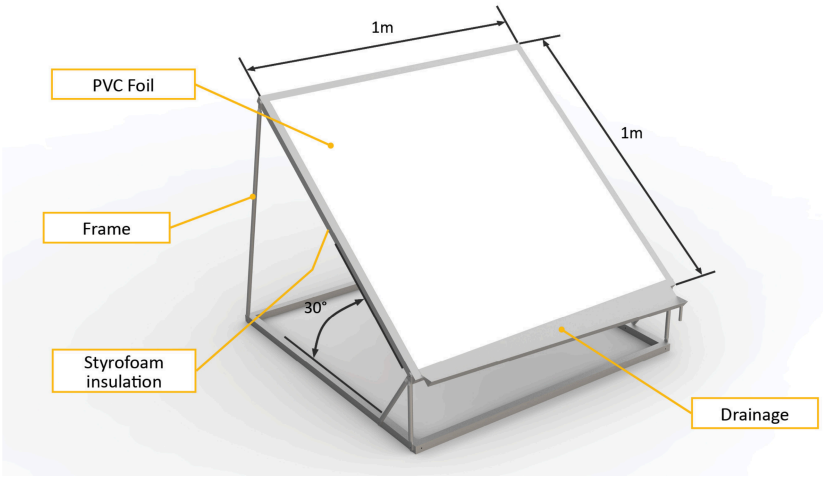


Figure 2. Schematic of the standard passive dew collector used in the Helsinki and Maktau field experiments. The setup consisted of a 1 m × 1 m PVC foil condenser mounted at a 30° inclination angle on an insulated frame, with 25 mm polystyrene foam insulation at the back and a drainage channel for passive water collection.

The Maktau site (3.43° S, 38.14° E), located in southeastern Kenya, represents a semi-arid tropical climate described by warm temperatures, seasonal rainfall, and frequent nocturnal radiative cooling under clear sky conditions. Measurements were conducted from 15 February 2016 to 31 March 2017 using three PVC condenser panels, installed at a 30° inclination angle with an insulated back, each with an area of 1 m^2. The panels were wiped every morning at sunrise at 6.00 AM. This dataset and the relevant findings have been previously reported by Tuure et al. [5].

The Ajaccio site (41.92° N, 8.74° E), located on the island of Corsica in the western Mediterranean, represents a coastal Mediterranean climate with mild winters, warm summers, and frequent nocturnal humidity from the sea. This experiment was dated from 22 July 2000 to 11 November 2001, and the dew observations were from a polymethyl methacrylate (PMMA) condenser surface with a horizontal collector plate. This dataset has been widely used in dew studies and is described by Beysens et al. [19].

The Bordeaux site (44.84° N, 0.58° W), located in southwestern France, represents a temperate oceanic climate influenced by the Atlantic Ocean. Measurements were conducted from 21 November 2001 to 14 January 2003 using a PMMA condenser surface similar to what was used in Ajaccio. In contrast, the condenser in this experiment was a different setup compared to other condensers used here; this setup had a horizontal collector plate of a 5 mm thick, 0.4 × 0.4 m^2 plate of Plexiglas/PMMA (polymethylmethacrylate) placed on a thermally isolated mount of an aluminum foil in contact with the plate and a 5 mm thick sheet of polystyrene foam beneath the foil [6]. The Bordeaux dataset provides a useful contrast to Mediterranean and continental sites and has also been reported by Beysens et al. [19].

In the field datasets, dew days were derived from measurable collected water and therefore depended on the collector design, drainage efficiency, and the detection of the measurement method (rain gauge). Because the model counts any positive simulated condensation as a condensation event, the number of simulated condensation days was not directly comparable to the number of field-observed dew days.

2.3. Meteorological and Climate Data

The meteorological input parameters for the dew condensation model were derived from the ECMWF ERA5 reanalysis dataset. ERA5 provides a spatially and temporally continuous representation of near-surface atmospheric conditions and has been widely

used in dew and non-rainfall water studies. In this study, ERA5 data were used as the main input for model simulations at all sites to ensure consistency across climatic regions.

ERA5 variables were extracted at the grid cell closest to each study site and included air temperature (at 2 m height), dew point temperature (at 2 m height), wind speed (at 10 m height), downward shortwave radiation, and downward longwave radiation as well as the surface roughness. Wind speed was calculated from the ERA5 zonal and meridional wind components (formulas are presented in Appendix A, Appendix A.2). All variables were used at an hourly temporal resolution and mapped directly to the corresponding model inputs described in Section 2.1.

Since the datasets did not include cloud coverage, the radiation variables were used instead to represent radiative forcing (energy imbalance between incoming solar energy and outgoing heat radiation) of the condenser surface without additional parameterization of cloud cover.

In addition to ERA5, on-site meteorological observations from local weather stations close to field experiments were used for comparison purposes. Weather station data were available for the sites located in Helsinki (Finland) and Maktau (Kenya), where the previous related dew collection field experiments were conducted [3–5]. In Helsinki, the meteorological variables temperature, relative humidity, wind speed, precipitation and shortwave solar radiation were logged on site by an automatic weather station (AWS) using a multiparameter weather transmitter (WXT530 Weather Transmitter Series, Vaisala, Vantaa, Finland) installed 1.9 m above ground in 1-min intervals [34]. The dewpoint was calculated using relative humidity and temperature via the Magnus formula [35] using expressions for the saturation vapor pressures over water or ice as given in [36]. The atmospheric longwave radiation was taken from the Kumpula weather station, Finnish Meteorological Institute (FMI), Helsinki, Finalnad, approximately 3 km away from the collector field setup. For Maktau, the longwave radiation was not available from the local weather station, and it was replaced with ERA5 values.

The field experiment results from Ajaccio and Bordeaux were compared directly to ERA5 simulation results. While at other sites (Helsinki and Maktau), weather stations data were aligned and compared with ERA5 data to enable direct comparison of meteorological parameters and resulting modelled dew yields vs. the field experiment dew yield.

All meteorological datasets were adjusted or interpolated as needed to match the model time step. Spatial interpolation was not applied beyond selection of the nearest ERA5 grid point to each site.

2.4. Climate Projection

Future dew formation was modelled using climate projection data from the Coordinated Regional Climate Downscaling Experiment (CORDEX) for the period 2027–2037. For the European study sites, simulations were taken from the EURO-CORDEX EUR-11 domain, which has a horizontal resolution of 0.11° (approximately 12.5 km) [32]. The selected dataset was based on the ICHEC-EC-EARTH global climate model, realization r12i1p1, under the RCP4.5 scenario, dynamically downscaled with REMO2015, and extracted at hourly temporal resolution from the CORDEX archive.

The meteorological parameters necessary for the dew model included near-surface air temperature, relative humidity (used together with air temperature to calculate dew point temperature), wind speed, downward shortwave radiation, and downward longwave radiation. Data from the nearest grid cell of each site was extracted and converted to the temporal resolution required by the model.

The same dew formation model described in Section 2.1 was applied using CORDEX data to estimate future changes in dew under projected climatic conditions. The results

were interpreted as estimates, with emphasis on relative changes in dew occurrence and yield rather than exact deterministic values of dew yield. Only one CORDEX model chain and one emission scenario were used, and therefore no multi-model analysis was carried out. This choice was also motivated by the requirement for hourly meteorological input for the dew model, which limited the number of suitable CORDEX datasets available for this application.

3. Results

3.1. ERA5 and Local Weather Data vs. Field Experiments

The comparison between modelled and observed dew yields showed that the model reproduced the progression of dew accumulation reasonably well, although the total yield of simulated and field observations did not match (Figure 3, Table 1). ERA5 simulations showed the largest cumulative bias at Helsinki and Maktau, with bias percentages of +176% in Helsinki 2022, +124% in Helsinki 2024, and +146% in Maktau (Table 1). The mismatch was smaller in Ajaccio (+17.9%), while Bordeaux showed underestimation (−18.8%). Correlation and error statistics further showed that agreement was strongest at Ajaccio and Bordeaux and weaker at Helsinki and Maktau (Table 1).

Table 1. Validation statistics for modelled daily dew yield compared with field observations at the five sites using ERA5 and local weather station data. Including the number of matched observations (n), Pearson correlation coefficient (r), coefficient of determination (R^2), root mean square error (RMSE), mean absolute error (MAE), mean bias error (MBE), and bias percentage. Positive MBE and bias values indicate model overestimation, whereas negative values indicate underestimation.

Site	Input Source	*n*	*r*	R^2	*RMSE*	*MAE*	*MBE*	*Bias (%)*
Helsinki 2022	ERA5	76	0.12	0.01	0.15	0.11	0.08	176
	Local	76	0.18	0.03	0.12	0.08	0.05	99
Helsinki 2024	ERA5	54	0.43	0.18	0.19	0.15	0.12	124
	Local	53	0.29	0.08	0.11	0.09	0.02	19
Maktau	ERA5	411	0.27	0.07	0.14	0.11	0.09	146
	Local	411	0.35	0.12	0.11	0.08	0.05	78
Ajaccio	ERA5	478	0.53	0.28	0.04	0.02	0.00	17
Bordeaux	ERA5	420	0.56	0.31	0.03	0.02	−0.01	−18

At the Helsinki site, both field experiments showed an overestimation by ERA5. During the 2022 campaign, observed cumulative (43 observed dew nights over 76 experimental days) dew reached 3.5 L m^{-2}, while ERA5 simulated 9.7 L m^{-2} (69 nights with simulated condensation), corresponding to 2.8 times the measured total (Figure 3a,b). While the use of local weather station data for the simulation reduced the cumulative estimate to 7.0 L m^{-2} (56 nights with simulated condensation) and improved agreement with observations. A similar pattern was found in the 2024 field test, where observed cumulative dew was 5.1 L m^{-2} (43 dew nights over 54 days of experiment) compared with 11.5 L m^{-2} from ERA5 (51 nights with simulated condensation) corresponding to 2.2 times higher, while local weather station produced 6.1 L m^{-2} (45 nights with simulated condensation) and showed much closer agreement with the field data (Figure 3c,d).

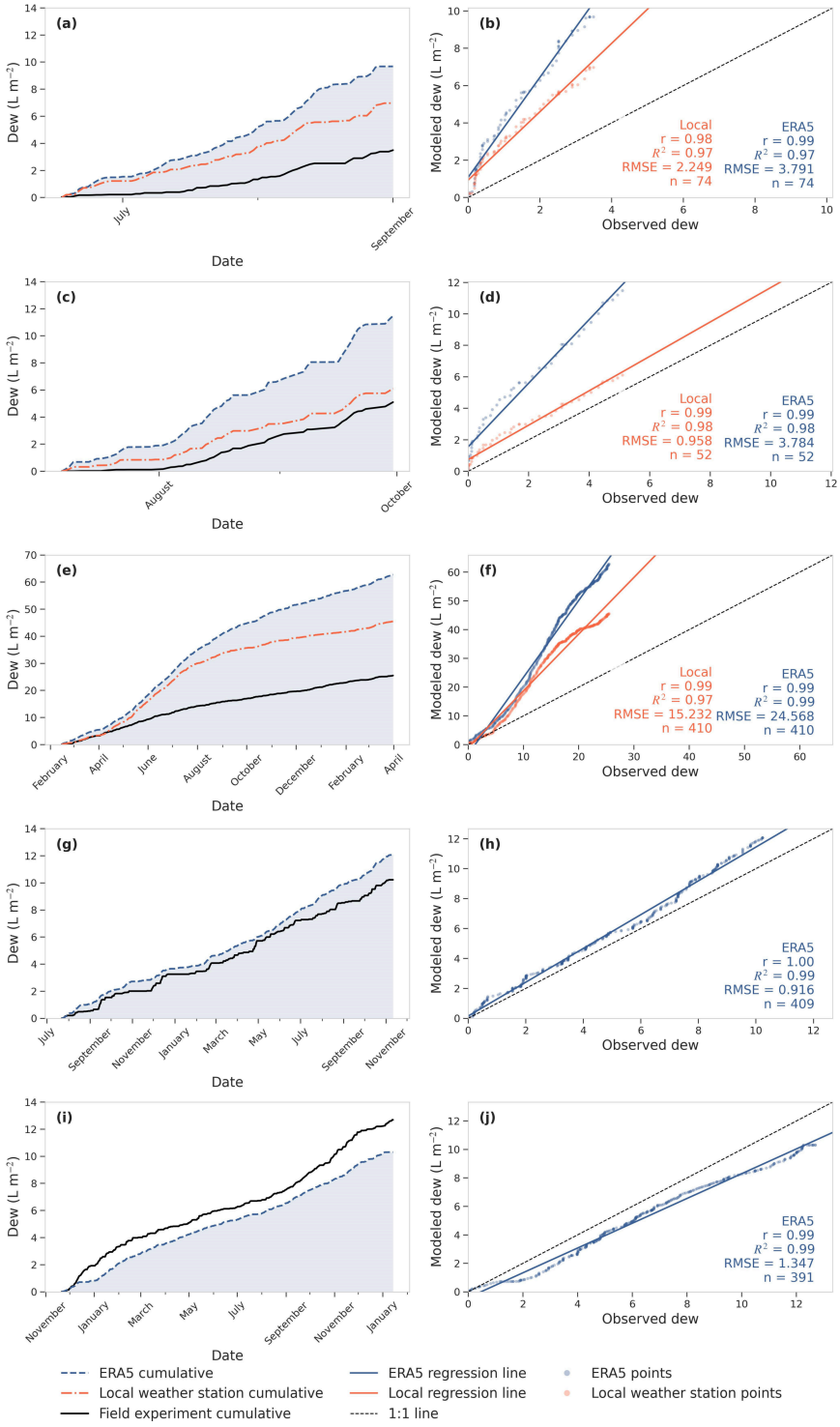


Figure 3. Comparison of observed and modelled cumulative dew yield using ERA5 and local weather station across the validation sites. Left panels show cumulative dew yield over the different observation periods, while right panels show cumulative agreement between modelled and observed dew with the 1:1 reference line. (**a**,**b**) Helsinki from 17 June to 31 August 2022; (**c**,**d**) Helsinki from 7 July to 30 September 2024; (**e**,**f**) Maktau from 15 February to 31 March 2017; (**g**,**h**) Ajaccio from 22 July 2000 to 11 November 2001; (**i**,**j**) Bordeaux from 21 November 2001 to 14 January 2003. Blue dashed lines indicate ERA5-driven simulations, orange dash-dotted lines indicate model runs by local weather station data, and black solid lines indicate field observations. Including the number of matched observations for cumulative dew yields (n), Pearson correlation coefficient (r), coefficient of determination (R^2), and root mean square error (RMSE).

The Maktau dataset showed the highest modelled cumulative totals among the sites. Observed dew accumulation (305 dew nights over 411 days of experiments) reached 25.5 L m^{-2}, while ERA5 simulated 62.8 L m^{-2} (405 nights with simulated condensation) and the local weather station 45.5 L m^{-2} (389 nights with simulated condensation) (Figure 3e,f). Although both simulated datasets overestimated the measured totals, the local station data again reduced the bias relative to ERA5.

For the long-term Mediterranean and Atlantic sites, only ERA5 was available. In Ajaccio, cumulative modelled dew (406 nights with simulated condensation in 478 experiment days) reached 12.1 L m^{-2} compared with 10.2 L m^{-2} observed (138 dew nights), representing an overestimation factor of 1.2 (Figure 3g,h). Bordeaux also showed relatively close cumulative agreement with a ratio of 0.81 and an amount of 12.0 L m^{-2} (372 nights with simulated condensation in 420 dew events) compared to 12.7 L m^{-2} (253 dew nights) for ERA5 and observed amount, respectively (Figure 3i,j).

The cumulative agreement plots further illustrate these differences (Figure 3b,d,f,h,j). ERA5 and local lines generally followed the same accumulation trajectory as field observations, but with steeper slopes at sites where total overestimation occurred. The closest match to the 1:1 reference line was observed for Ajaccio and Bordeaux, whereas Helsinki and Maktau showed larger deviations, particularly for ERA5.

A sensitivity test using neighboring ERA5 grid cells showed that the effect of grid-cell selection varied between sites (Appendix B, Figure A2). At Bordeaux, the cumulative simulated dew curves from the neighboring grid cells were relatively similar, indicating only limited variation in cumulative dew yield. In contrast, at Helsinki the spread between neighboring grid cells was larger, with northern and southern cells producing different cumulative totals. The largest differences were observed where adjacent grid cells differed in land–water influence.

A comparison of hourly ERA5 and local weather station input data during the dew events (Appendix B, Table A1) showed differences between the two datasets, particularly in wind speed and dew point temperature. Differences were also present in shortwave radiation during the early morning hours.

The daily time series made clear the differences between the field experiment's dew and modelled dew events across the five datasets (Figure 4). ERA5 and local weather station simulations showed the general timing of dew events. Still, they often produced more frequent and more uniform daily condensation events than were observed in the field. This was most clear at Helsinki and Maktau, where the model predicted dew on many days with little or no measured accumulation in the field setup.

At Helsinki 2022, both ERA5 and local weather station simulations showed repeated daily dew events throughout the experiment, with ERA5 producing the highest values (Figure 4a). The field observations were more irregular, with several zero dew nights between events and fewer continued periods of condensation. A similar pattern was found for Helsinki 2024 (Figure 4b), where both modeled datasets followed the general temporal variability of the field observations, while the local weather station simulation was closer in magnitude.

The Maktau dataset showed the uninterrupted dew events of daily modelled dew among all sites (Figure 4c). Both ERA5 and local weather station simulations produced continuous daily condensation over the observation period, whereas the field observations showed larger short-term variability (ranging from 0 to approximately 0.34 L m^{-2} d^{-1}) and more frequent drops to very low values (<0.02 L m^{-2} d^{-1}) or zero.

For Ajaccio and Bordeaux, where only ERA5-driven simulations were available, the daily comparisons showed different behavior. In Ajaccio, the ERA5 series was continuous and low to moderate in magnitude, while the observed field data were more irregular and

characterized by sharper peaks separated by zero or near-zero (<0.02 mm day^{-1}) days (Figure 3d). In Bordeaux, ERA5 simulated the overall seasonal progression well, but it still showed stronger day-to-day irregularity and higher short-term peaks than the modelled values (Figure 4e).

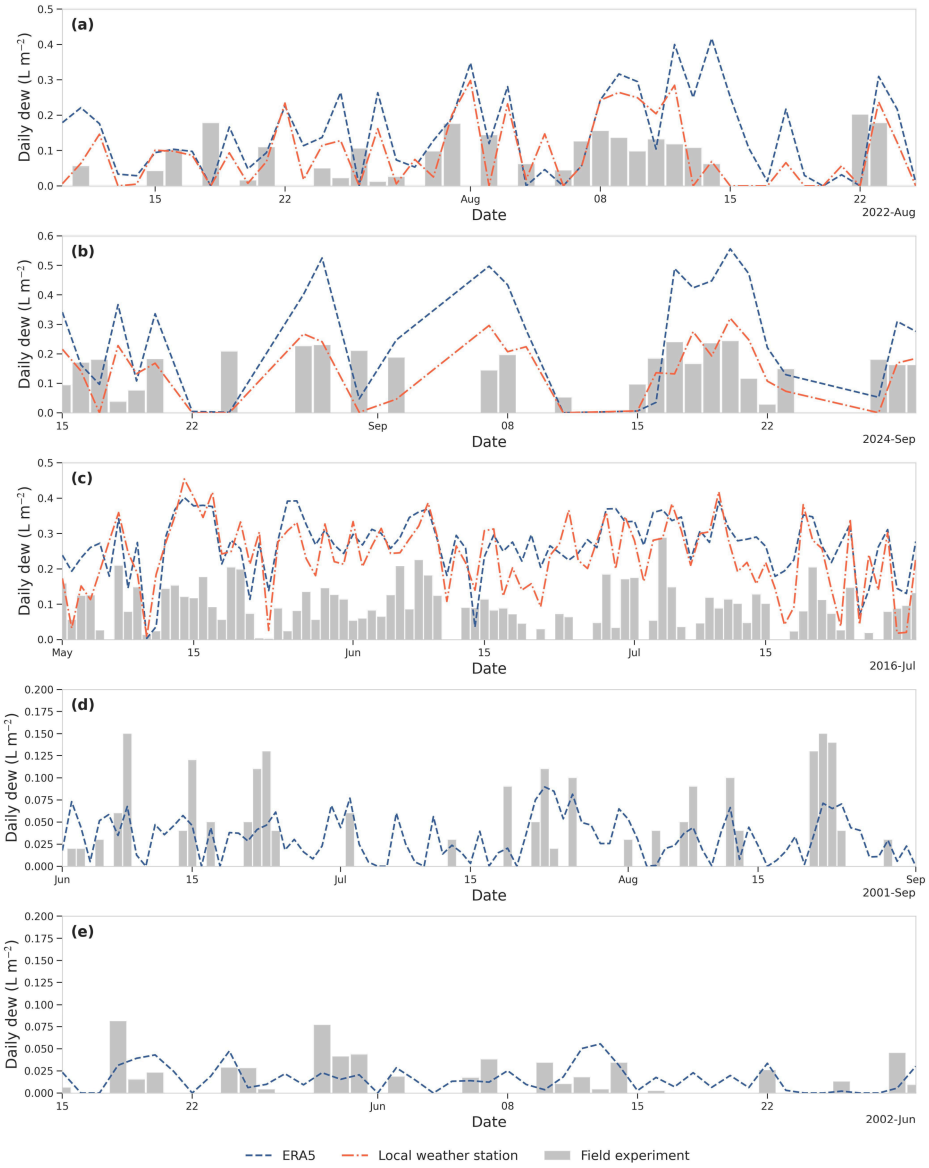


Figure 4. Daily observed and modelled dew yield for the validation datasets. (**a**) Helsinki 2022, (**b**) Helsinki 2024, (**c**) Maktau 2016–2017, (**d**) Ajaccio 2000–2001, and (**e**) Bordeaux 2001–2003. Blue dashed lines show ERA5 model output, orange dash-dotted lines show simulations with local weather station data, and grey bars show field observations of dew amount.

3.2. Climate Projection of Dew Formation Under CORDEX Dataset

Modeled projected dew formation from CORDEX climate data showed clear differences among the three European study sites (Figure 5). Bordeaux consistently showed the highest modelled dew yields throughout the projection period, followed by Helsinki, while Ajaccio showed the lowest dew accumulation.

In this section, "days with simulated condensation" refers to any day with positive modelled condensate accumulation and should not be interpreted as directly equivalent to field-observed dew days.

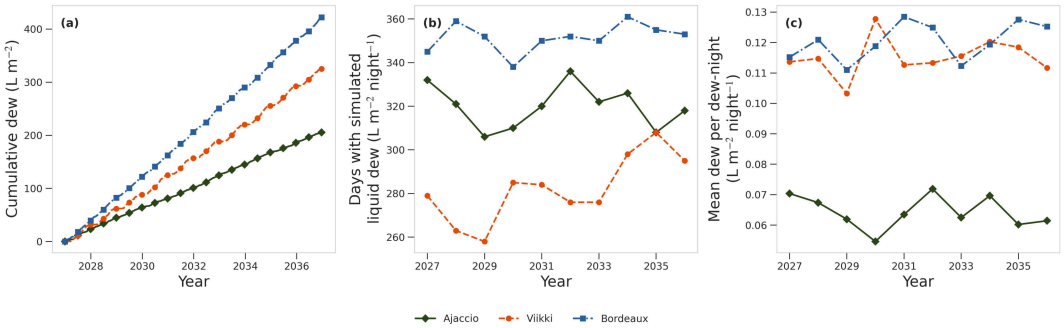


Figure 5. Projected dew formation under CORDEX climate forcing for the three European study sites (Ajaccio, Helsinki, and Bordeaux) during the forecast study period of 11 years (January 2027–December 2037). (**a**) Cumulative modelled dew yield (L m^{-2}) showing progressive accumulation over time. (**b**) Number of days with simulated condensation per year (L m^{-2} $night^{-1}$). (**c**) Mean dew yield per night with simulated condensation (L m^{-2} $night^{-1}$).

Cumulative modelled dew yield increased steadily over time at all sites (Figure 5a). By the end of the projection period, cumulative totals reached approximately 423 L m^{-2} in Bordeaux, 325 L m^{-2} in Helsinki, and 205 L m^{-2} in Ajaccio for a period of 11 years. The higher cumulative values in Bordeaux reflect both higher annual dew totals and more frequent nights with dew compared with the other locations.

Annual modelled dew yield varied annually but remained relatively stable overall (Figure 4b). Mean annual dew yield was highest in Bordeaux at 42.3 L m^{-2} yr^{-1}, followed by Helsinki at 32.5 L m^{-2} yr^{-1} and Ajaccio at 20.6 L m^{-2} yr^{-1}. Annual values ranged from 39.1 to 45.3 L m^{-2} yr^{-1} in Bordeaux, 26.6 to 36.5 L m^{-2} yr^{-1} in Helsinki, and 16.9 to 24.2 L m^{-2} yr^{-1} in Ajaccio.

Trend analysis indicated no statistically significant monotonic trend in annual dew yield at any site during the analyzed period (Figure 5b). Sen's slope estimates were slightly positive for Bordeaux (+0.48 L m^{-2} yr^{-1}) and Helsinki (+0.42 L m^{-2} yr^{-1}), while Ajaccio showed a weak negative slope (−0.20 L m^{-2} yr^{-1}).

The number of days with simulated condensation per year also varied among locations (Figure 5c). Bordeaux had the highest frequency, averaging 352 days with simulated condensation yr^{-1}, followed by Ajaccio with 320 days yr^{-1} and Helsinki with 282 days yr^{-1}. Bordeaux remained above 338 days with simulated condensation yr^{-1} in all years, indicating highly persistent dew occurrence, whereas Helsinki showed greater annual variability, ranging from 258 to 309 days with simulated condensation yr^{-1}.

Mean dew yield per night with simulated condensation was highest in Bordeaux (0.120 L m^{-2} $night^{-1}$) and Helsinki (0.115 L m^{-2} $night^{-1}$), while Ajaccio showed lower nightly condensation (0.064 L m^{-2} $night^{-1}$) (Figure 5c). Interannual variability in annual dew totals was lowest in Bordeaux (coefficient of variation = 5.8%), followed by Helsinki (9.4%) and Ajaccio (11.2%), suggesting that projected dew formation was most stable in Bordeaux and most variable in Ajaccio over the study period.

The year-by-year cumulative dew curves made it clear how seasonal dew progresses as well as presenting the distribution of condensed dew throughout the projected period for three European sites (Figure 6). In Ajaccio, cumulative dew increased gradually throughout the year, with a median annual total of 20.2 L m^{-2} yr^{-1} and a range of 16.9–24.2 L m^{-2} yr^{-1} (Figure 6a). In Helsinki, accumulation remained low during the early part of the year and then increased more rapidly from spring onward, reaching a median annual total of 31.9 L m^{-2} yr^{-1} with a range of 26.6–36.5 L m^{-2} yr^{-1} (Figure 6b). Bordeaux showed the highest and most uniform cumulative accumulation, with a steady increase across the year and a median annual total of 43.2 L m^{-2} yr^{-1} (range 39.1–45.3 L m^{-2} yr^{-1}; Figure 5c).

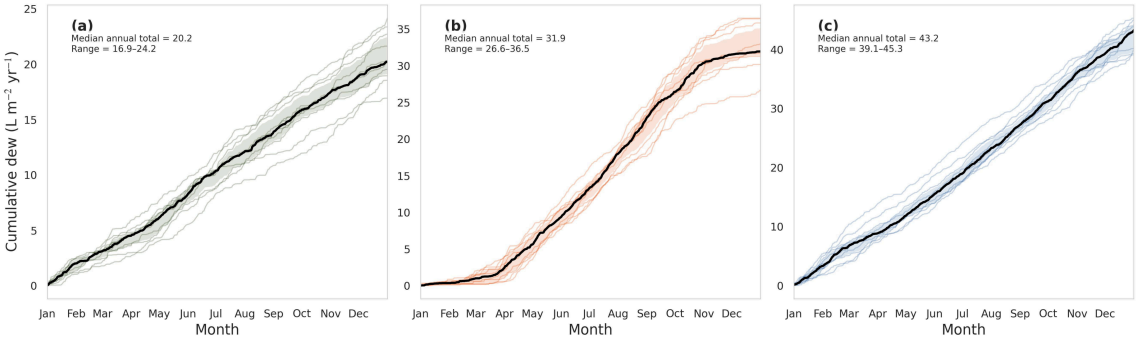


Figure 6. Year by year cumulative dew curves under CORDEX climate forcing for the forecast period of 11 year, with the median cumulative curve shown in black and colored lines represents the induvial years range for each sites. (**a**) Ajaccio. (**b**) Helsinki (**c**) Bordeaux. Thin colored lines represent individual projected years, and the text inset in each panel shows the median annual total and annual range (L m^{-2} yr^{-1}).

Daily projected liquid dew and ice deposition in 2027 illustrated the seasonal differences among the sites (Figure 7). In Ajaccio, liquid dew was collected during most months of the year, while ice deposition was mainly visible during winter and late autumn periods (Figure 7a). In Helsinki, liquid dew was visible between late spring and autumn, whereas ice deposition was frequent during the colder months at the beginning and end of the year (Figure 7b). Bordeaux showed liquid dew throughout the year, with frequent daily events, while ice deposition occurred during colder periods (Figure 7c).

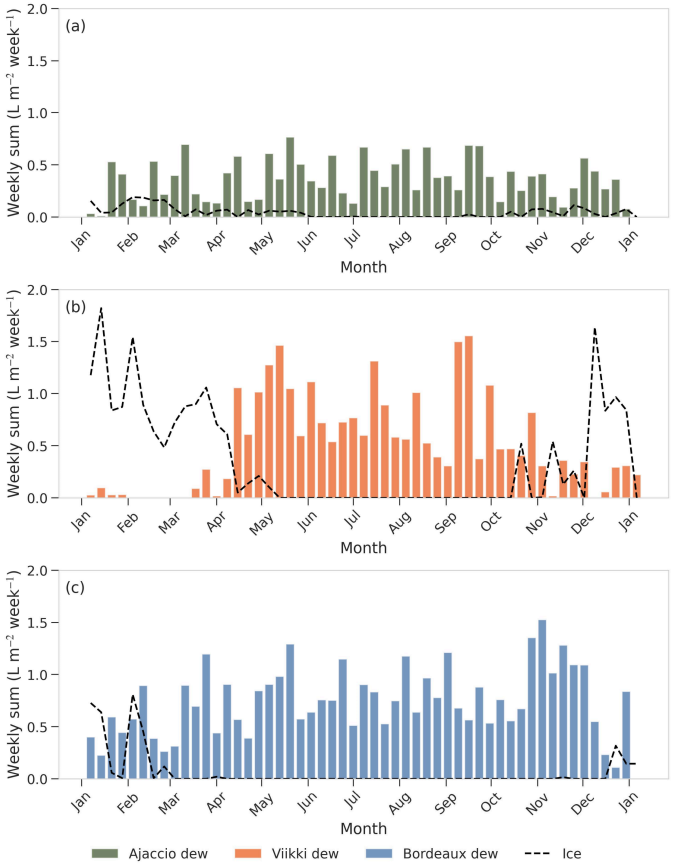


Figure 7. Weekly summed modelled liquid dew and ice deposition in 2027 for the three projected study sites. (**a**) Ajaccio. (**b**) Helsinki; (**c**) Bordeaux. Colored bars show weekly liquid dew yield, while the black dashed line shows weekly ice deposition. The weekly aggregation is used to highlight the seasonal variation in condensation more clearly.

4. Discussion

4.1. Model Performance with ERA5 and Local Weather Data

The comparison between modelled and observed dew yields showed that the model simulated the general timing of dew accumulation correctly, but its performance varied among sites and different datasets (i.e., ERA5 vs. local weather station). In most cases, the model overestimated cumulative dew yield, particularly at Helsinki and Maktau; however, the agreement was closest at Ajaccio and Bordeaux. This pattern suggests that the model is more successful in reproducing the overall condensation potential than the exact amount of dew collected under field conditions. Part of the discrepancy in event frequency is also because the model counts any positive simulated condensation as an event, whereas field observations reflect measurable collected dew only.

A possible reason for this discrepancy could be related to how the model represents the condenser surface and the condensation process itself. The model assumes a horizontal condenser sheet thermally insulated from the ground, which enhances radiative cooling and favors condensation [28]. In contrast, the field collectors at Helsinki and Maktau are standard dew collectors which were installed at a 30° inclination to optimize passive drainage/collection rather than maximum radiative cooling [20,37].

It is worth mentioning that a sensitivity test for Collector inclination was not tested separately in this study, because the model does not explicitly represent tilt angle. Therefore, the mismatch between the horizontal model surface and the 30° field collectors should be considered an important limitation in the model field comparison.

This difference in geometry is important because an inclined surface exchanges radiation and heat differently than a flat insulated sheet and may therefore cool less efficiently under real conditions [14,20,28]. By comparison, the Ajaccio and Bordeaux dew observations were made on horizontal PMMA condensers serving as a reference for larger inclined collectors [6,19], which are more aligned with the model assumption.

This likely contributed to the closer agreement between observed and modelled dew yields for Ajaccio and Bordeaux, although the match was still imperfect. For example, the Bordeaux condenser was a horizontal PMMA plate similar in orientation and material to the model assumption, but its smaller size (0.16 m^2 rather than 1 m^2) may have affected edge effects, thermal inertia, and therefore the condensation behavior [14,20]. Therefore, the better agreement at Ajaccio and Bordeaux should be interpreted as relative rather than as evidence that the experimental setup fully matched the model assumptions. Moreover, the accumulated dew on these horizontal condensers was measured by weighing [6,19]. For the inclined condensers, the dew was collected passively, assisted by gravity. Considerable amounts of dew droplets were pinned to the condenser surface, thus uncollected [3,4].

Part of the remaining discrepancy may also be related to uncertainty in the ERA5 input data itself. ERA5 provides hourly data at about 31 km spatial resolution and includes an estimate of the relative random uncertainty, but this does not represent absolute or systematic uncertainty [38]. In addition, ECMWF notes that analysis accuracy was not uniform within each window and depended on the parameter and location [39].

The neighboring grid sensitivity analysis indicated that uncertainty related to ERA5 grid-cell selection was site dependent. At Bordeaux, where the grid cells produced similar cumulative dew curves, the effect of grid selection appears small. At Helsinki, however, the larger spread among neighboring cells suggested that the presence of local land water could influence the data and, consequently, the simulated dew yield. This supports the use of the nearest ERA5 grid cell as the most reasonable representation of site conditions, while also showing that spatial representation remains an additional source of uncertainty, especially at mixed coastal or land water sites.

However, for a dew collector, using the nearest ERA5 grid cell unavoidably smooths gradients in wind, humidity, radiation, and land surface characteristics, which may be important at mixed sites such as Ajaccio and Bordeaux. Therefore, part of the mismatch between modelled and observed dew may arise not only from the dew model itself, but also from the spatial representativeness and uncertainty of the ERA5 meteorological input.

A comparison of hourly ERA5 and local weather station input data during a representative dew event (Appendix B, Table A1) showed clear differences between the two datasets, particularly in wind speed and dew point temperature. Because these variables directly influence condensation rate and surface cooling, such differences likely contributed to the mismatch between modelled and observed dew yields and may help explain why local weather station data often improved agreement relative to ERA5.

Another possible source of deviation was that the model accumulates condensation whenever meteorological conditions were thermodynamically favorable but does not include evaporation of condensed dew and represent the interruption and recovery of condensation under rapidly changing field conditions [28,30,40]. In reality, dew condensation is, however, highly sensitive to short-term fluctuations in wind, cloud cover, and near-surface humidity [7]. For example, an increase in wind speed may temporarily enhance turbulent air mixing and warming of the condenser surface, while other parameters such as cloud cover can reduce net radiative loss by increasing incoming longwave radiation.

At Helsinki, part of the condensed water may also have evaporated after sunrise as the collector surface warmed and relative humidity decreased, especially during low-yield events. More generally, this effect is expected to amplify under conditions of increasing wind speed, rapid surface warming, and declining humidity after dawn [7,40]. Because the model defines daily dew as the maximum accumulated condensed water and does not account for post-sunrise evaporation, this process may have contributed to the observed overestimation of harvested dew under field conditions.

The cumulative and daily comparisons showed two different patterns. At some sites, the total dew amount modeled by ERA5 or local weather station data was close to the amount measured in the field, but the daily event pattern still did not match well.

More specifically, the model predicted dew over more days than were observed. For example, at Helsinki in 2022, 43 dew days were recorded in the field, whereas the ERA5- and local weather station simulations produced 69 and 56 dew days, respectively. This suggests that the model allows condensation under a broader range of conditions than those that resulted in measurable or harvestable dew in the field.

A similar effect was also observed at Ajaccio and Bordeaux, where cumulative agreement between ERA5 and field observations was relatively close, but this agreement was not present in daily basis. In such cases, the model may reproduce the total accumulated dew over a long period while still differing in the number of dew-forming days and the intensity of individual events. Therefore, close cumulative agreement should not be interpreted as exact agreement on the day-to-day scale [8,27,28].

The use of local weather station data improved the agreement in some cases, but not consistently. In Helsinki 2022 and to a larger extent at Helsinki 2024, local data reduced cumulative overestimation vs. the ERA5, indicating that local meteorological observations better represented site-specific nocturnal conditions and reduced the uncertainty of the ERA5 meteorological input and the spatial resolution. However, although local weather data could produce more accurate estimation, the general bias of the model toward overestimation remains.

In the case of Maktau, this improvement should be interpreted with caution because the local weather station data simulation was partly hybrid: longwave radiation was not available from the local weather station, and ERA5 longwave radiation was used instead.

Thus, the improved agreement suggests that the local near-surface variables, especially air temperature, humidity/dew point, and wind speed, likely reduced part of the error, although the simulation was not fully independent of ERA5.

So rather than focusing on the accuracy of the weather data, the focus should be shifted toward the condensation process; e.g., even when local temperature, humidity, and wind observations are available, the total collected water from the condenser surface still depends on processes such as air flow at the condensing surface, droplet retention, delayed runoff, re-evaporation, local sheltering, and surface wetting history [7].

Material and surface condition effects were perhaps another likely source of disagreement between modelled and observed dew. The model includes adjustable condenser properties, including emissivity, sheet thickness, and insulation [28], but these parameters do not fully capture the complexity of real field collectors.

Under field conditions, condensation is also controlled by surface tilt, passive droplet drainage/collection, surface wettability, local shielding from wind, and short-term changes in surface wetness [20–22], all of which directly affect how efficiently condensed water is collected. As a result, even with realistic material parameter values, the model may still represent the thermodynamic potential for condensation better than the actual harvested amount [28]. This may help explain why the agreement was better for Ajaccio and especially Bordeaux, where the flat PMMA setup was closer to the model assumptions, than for the tilted PVC panel experiments in Helsinki and Maktau.

The results indicate that the model is perhaps most reliable for representing relative and cumulative dew potential in both short term (four-five months of Helsinki sites) and long term (plus one year period in Maktau, Ajaccio and Bordeaux), but less accurate for exact harvested amounts and daily event occurrence under field conditions. The strongest agreement was obtained for flat PMMA datasets in Ajaccio and Bordeaux, where the experimental setup most closely resembled the modelled condenser geometry and surface type while larger mismatches remained for the tilted PVC or standard panel experiments at Helsinki and Maktau. Highlighting the importance of collector design, local meteorological variability, and droplet relations to the condenser that are not represented in the model.

4.2. Projected Dew Formation Under CORDEX Climate Data

The CORDEX-based analysis was intended to test whether near-future climate data can replicate realistic dew seasons, relative site differences, and short-term changes in dew potential, rather than predicting the exact future harvestable dew amounts. This is important because, as shown in the ERA5 and local weather station evaluation, the model tends to simulate more condensation potential than the actual amount of water that can be collected in the field [27,28]. In that sense, the CORDEX results could be useful for interpreting seasonal behavior and comparing site differences under different climate conditions [31].

Similar to ERA5 data, the CORDEX also presents uncertainty in its data. Although regional climate simulations provide finer spatial detail (for European study sites used in this study, the resolutions were 0.11° or 12.5 km) than global models, they still inherit biases from the driving global climate models and remain affected by uncertainty related to emission scenarios, internal climate variability, model configuration, and the choice of downscaling method [32,41,42]. These sources of uncertainty are relevant on shorter time scales such as the 2027–2037 period used here, where internal variability can affect the development of any trend signal.

In addition, because only one EURO-CORDEX model chain under one emission scenario was used, the projected dew estimates do not capture inter-model or inter-scenario

spread and should therefore be interpreted as a single-chain near-future estimate rather than a full ensemble-based climate projection.

Therefore, the results were interpreted primarily from a validation perspective, with emphasis on relative site differences, the accuracy of dew season occurrence, and short-term trends, rather than on the absolute projected magnitude of future dew yield.

The projected model results showed different condensation behavior for the three European sites. This is an important validation point for models, especially where similar model structure and climate input have been used. More specifically, the sites showed different condensation behavior, which showcases the influence of local climate on both dew frequency and nightly yield. Bordeaux was characterized by the highest and most stable condensation potential; Ajaccio showed frequent but generally weak condensation, and Helsinki had a seasonal condensation regime with high-intensity events when conditions were favorable.

Looking further into the sites, Bordeaux's projected behavior was consistent with its oceanic setting and strong maritime influence. The combination of high annual totals and many nights with simulated condensation suggested that favorable condensation conditions remain available during most of the year. Bordeaux represents a climate where the model projects constant condensation rather than a short dew season, which is consistent with a previous study at the site [19].

Ajaccio results were consistent with a Mediterranean coastal climate, where humidity supply from the sea can support frequent condensation, while warmer night-time conditions and greater ventilation may reduce the radiative cooling needed for stronger dew formation [6,43]. This, in turn, is shown directly as a high number of dew nights in the model prediction but at the same time as a lower annual total, which indicates that it had less frequent high-amount dew events.

Helsinki behaved as a site where annual dew totals depend more on the duration and timing of the dew season than on year-round condensation. Considering how seasonal the dew collection is in Finland; such result from the model projection seems realistic [3,4]. Although the annual totals of Helsinki remained below Bordeaux, the nightly yields were similar when condensation occurred, indicating that the site was capable of efficient dew formation during favorable periods. Therefore, the main limitation was the short dew season window in which dew could form. This is clear on the cumulative curve where accumulation remains limited for part of the year and then increases rapidly during the main dew season.

The differences in dew season among the three sites were also clear in the daily time series. Bordeaux showed liquid dew during most of the year, interrupted only during colder periods, which matches the high projected number of days with simulated condensation. Ajaccio also showed relatively continuous occurrence, but with smaller daily amounts, again supporting the interpretation of frequent but mostly weak condensation. Helsinki, by contrast, showed a clear dew season from late spring to autumn, with very limited liquid dew during winter and early spring. This seasonal pattern is consistent with the known dew season in Finland and with the stronger role of cold-season frost and ice formation at northern sites [2,3].

Helsinki projection highlighted the importance of models simulating ice on the condenser surface. During the colder parts of the year, condensation frequently occurred as ice rather than liquid dew, especially during the beginning and end of the dew season i.e., spring and autumn transitions. This is also reflected in the cumulative curves, where accumulation remains low during winter and then rises more rapidly once liquid dew becomes dominant. Such overlap between dew and ice is physically realistic, because the water forming on the collector surface may freeze when the surface remains below

0 °C [7,16]. The model therefore suggests that condensation potential in Helsinki is not absent outside the liquid-dew season but partly shifted into frozen deposition [28].

The projected year-to-year changes should also be interpreted mainly as directional rather than climatic trends. Helsinki showed the clearest positive direction in both annual condensation amount and frequency of days with simulated condensation, while Bordeaux showed only a weak positive direction around the baseline, and Ajaccio showed a slight negative tendency. Since the Mann–Kendall test did not indicate statistically significant monotonic trends, these changes should not be interpreted as robust long-term climate signals.

However, within the short 11-year window, they still provide useful information on how the modeled dew seasons may shift under near-future climate data. In that sense, the increasing direction in Helsinki suggests that the projected dew season may become longer or more favorable, while Bordeaux remains suitable and Ajaccio remains relatively stable but weak.

Altogether, the cumulative and daily projections show that annual dew totals alone are not sufficient for comparing site behavior. Bordeaux, Ajaccio, and Helsinki each reached their annual totals through different seasonal pathways: steady year-round accumulation in Bordeaux, gradual but weak accumulation in Ajaccio, and a shorter but more efficient seasonal window in Helsinki (Figures 5 and 6). This means that dew season timing, event intensity, and the phase of condensation (liquid or ice) are essential for interpreting projected dew behavior across climates.

The CORDEX simulations suggest that near-future dew potential remains noticeable across diverse European climates, but with distinctly different modes of occurrence: highly persistent and stable in Bordeaux, frequent but low-intensity in Ajaccio, and strongly seasonal with efficient events and partial ice overlap in Helsinki.

5. Conclusions

This study evaluated a model simulation-based dew formation across different climate conditions using field observations from Helsinki, Maktau, Ajaccio, and Bordeaux, together with ERA5, local weather station data, and near-future CORDEX climate projections.

The findings of this study indicated that ERA5 and local weather station data were both able to capture the overall progression of condensation, while local observations generally reduced cumulative bias in Helsinki by better representing site-specific nocturnal climate conditions.

CORDEX simulations used to examine relative future dew behavior were useful for comparing dew potential across different climates, replicating the general timing and cumulative development of dew events, and identifying dew seasons and short-term directional changes under projected climate data; the results are still valuable insights even when the aim is not absolute values of yield prediction.

Overall, the results showed that to achieve an accurate estimation of harvestable dew, the model needs a better representation of collector geometry and orientation, as the closest agreement was found for the flat PMMA collector datasets at Ajaccio and Bordeaux, while larger deviations were for the inclined standard collectors at Helsinki and Maktau.

Improved representation of condenser surface characteristics, surface wetting, drainage processes, and short-term local atmospheric variability would also be needed for more accurate yield estimation.

Author Contributions: Conceptualization, S.M.Z.K., J.T., S.G., T.H., N.A., P.P. and L.A.; methodology, S.M.Z.K., J.T., S.G., N.A. and T.H.; software, S.M.Z.K., J.T., S.G., N.A. and J.H.; validation, S.M.Z.K., J.T. and S.G.; formal analysis, S.M.Z.K., J.T. and S.G.; investigation, S.M.Z.K., S.G. and J.T.; resources, J.T., L.A., P.P., T.H. and S.G.; data curation, S.M.Z.K.; writing original draft preparation, S.M.Z.K.;

writing review and editing, all authors; visualization, S.M.Z.K. and S.G.; supervision, J.T., S.G. and L.A.; project administration, J.T. and L.A.; funding acquisition, J.T., L.A. and S.G. All authors have read and agreed to the published version of the manuscript.

Funding: This research was funded by Maa- ja vesitekniikan tuki ry (MVTT) and the University of Helsinki, grant number 4767.

Data Availability Statement: Data are available upon request.

Acknowledgments: We acknowledge financial support for this work from Maa- ja vesitekniikan tuki ry (MVTT) and the University of Helsinki. We also express our gratitude to Daniel Beysens for providing the field experiment datasets from Ajaccio and Bordeaux. The field experiment in Maktau, Kenya, was conducted under research permit P/18/97336/26355 from the National Council for Science and Technology of Kenya, which is gratefully acknowledged. We also thank the Taita Research Station of the University of Helsinki for logistical support during the Maktau fieldwork.

Conflicts of Interest: The authors declare no conflict of interest.

Abbreviations

The following abbreviations are used in this manuscript:

AWS	Automatic Weather Station
CORDEX	Coordinated Regional Climate Downscaling Experiment
ECMWF	European Center for Medium Range Weather Forecast
ERA5	Fifth generation ECMWF atmospheric reanalysis
PMMA	Polymethyl methacrylate
PVC	Polyvinyl chloride

Appendix A

Appendix A.1

Full formulation of the dew formation model, including radiative, convective, latent heat, and mass transfer equations.

The temporal evolution of the condenser temperature T_c is governed by the heat balance equation presented in the main text Formula (1), while the condenser mass is defined as:

$$m_c = \rho_c S_c \delta_c, \tag{A1}$$

where ρ_c is the condenser material density (kg/m^3), S_c is the surface area (1 m^2), and δ_c is the sheet thickness.

Radiative heat exchange:

The net radiative power P_{rad} is calculated as:

$$P_{\text{rad}} = (1 - a) S_c R_{sw} + \varepsilon_c S_c R_{lw} - P_c, \tag{A2}$$

where a is the surface albedo, ε_c is the longwave emissivity of the condenser, and R_{sw} and R_{lw} are the incoming shortwave and longwave radiation, respectively. The longwave emitted radiation from the condenser surface is

$$P_c = \varepsilon_c S_c \sigma T_c^4, \tag{A3}$$

where σ is Stefan Boltzmann constant.

Conductive and convective heat exchange:

Conductive heat exchange with the ground is neglected, as the condenser is assumed to be thermally insulated:

$$P_{\text{cond}} = 0. \tag{A4}$$

Convective heat exchange between the condenser and ambient air is expressed as:

$$P_{\text{conv}} = S_c h(T_a - T_c), \tag{A5}$$

where T_a is the air temperature at 2 m height and h is the convective heat transfer coefficient. Following Vuollekoski et al., h is parameterized as a function of wind speed at 2 m height using the formulation proposed by Richards et al., [25]:

$$h = 5.9 + 4.1u\left(\frac{511 + 294}{511 + T_a}\right), \tag{A6}$$

where u is the horizontal wind speed at 2 m height (m s^{-1}) and T_a is expressed in degrees Celsius.

Latent heat and condensation:

Latent heat release associated with condensation is given by:

$$P_{\text{lat}} = \begin{cases} L_{vw}\frac{dm_w}{dt}, & T_c \geq 0\ ^\circ\text{C}, \\ L_{vi}\frac{dm_i}{dt}, & T_c < 0\ ^\circ\text{C}, \end{cases} \tag{A7}$$

where L_{vw} and L_{vi} are the latent heats of vaporization and desublimation, respectively. Phase changes between liquid water and ice are handled by constraining the surface temperature to 0 °C during freezing or melting, as described by Vuollekoski et al.

The mass transfer coefficient k is related to the convective heat transfer coefficient by:

$$k = \frac{0.622h}{C_a p}, \tag{A8}$$

where C_a is the specific heat capacity of air and p is atmospheric pressure.

The model integrates Equations (A1)–(A8) over time and tracks the cumulative mass of condensed water and ice. Daily dew yield is defined as the maximum accumulated condensate within a diurnal cycle. Evaporation of condensed water during daytime is not considered, assuming that dew is collected shortly after sunrise. Fog deposition, precipitation, and surface wetting by non-condensational processes are not explicitly simulated. These assumptions are consistent with previous applications of the model [27,28] and allow consistent comparison across different climatic regions.

Appendix A.2

Wind speed calculation through ERA5.

Wind speed was derived from the ERA5 10 m zonal and meridional wind components as:

$$U_{10} = \sqrt{u_{10}^2 + v_{10}^2} \tag{A9}$$

where u_{10} and v_{10} are the ERA5 10 m U and V wind components, respectively. ERA5 provides these variables directly as standard single-level parameters.

To obtain the 2 m wind speed required by the dew model, the 10 m wind speed was converted using a logarithmic wind profile in Equation (A12):

$$u_2 = \frac{\log\left(\frac{2+z_0}{z_0}\right)}{\log\left(\frac{10+z_0}{z_0}\right)} U_{10} \tag{A10}$$

where z_0 is the surface roughness length extracted from ERA5 and used in the logarithmic wind profile conversion.

Appendix B

Table A1. Example comparison of hourly meteorological input variables from ERA5 and local weather station data during a representative dew event at Helsinki (20–21 August 2024). Variables shown are air temperature, dew point temperature, wind speed, shortwave radiation, and ERA5 surface roughness. The table illustrates differences between reanalysis and local forcing data used in the dew model calculations.

Date and Time	Air Temp. (°C)		Dew Point (°C)		Wind Speed (m/s)		Shortwave Radiation (W/m^2)		Surface Roughness
	ERA5	Local	ERA5	Local	ERA5	Local	ERA5	Local	ERA5
20-08-2024 21:00	13.8	13.7	12.6	11.21	1.6	0.2	0	0	0.7
20-08-2024 22:00	14.3	12.3	13.1	10.78	1.7	0.2	0	0	0.7
20-08-2024 23:00	14.2	12.1	13.1	10.82	1.7	0.2	0	0	0.7
21-08-2024 00:00	14.0	12.9	12.9	11.75	1.7	0.4	0	0	0.7
21-08-2024 01:00	13.8	15.6	12.7	13.56	1.6	0.9	0	0	0.7
21-08-2024 02:00	13.5	15.5	12.5	12.79	1.6	0.9	0	0	0.7
21-08-2024 03:00	13.4	14.0	12.5	11.86	1.4	0.4	0	0	0.7
21-08-2024 04:00	14.4	13.2	13.3	11.71	1.5	0.6	33.4	0	0.7
21-08-2024 05:00	16.2	12.0	14.5	10.72	1.6	0.2	119.7	0	0.7
21-08-2024 06:00	18.0	12.1	15.1	10.98	1.9	0.2	224.7	24	0.7

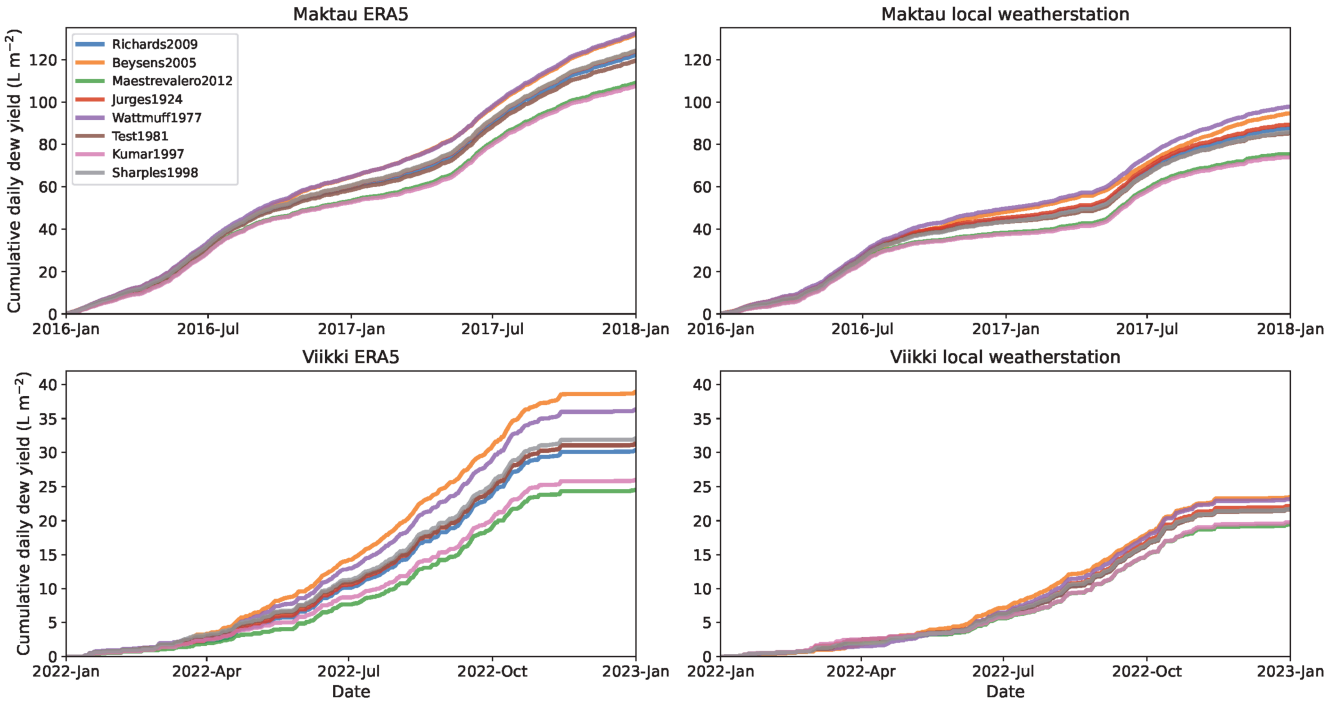


Figure A1. Sensitivity of cumulative simulated dew yield to alternative heat-transfer parameterizations affecting the mass transfer coefficient k, shown for Maktau and Helsinki (Viikki) using ERA5 and local weather station forcing. Although cumulative totals differ among parameterizations, the overall seasonal progression remains similar. The formulations shown correspond to Richards [25], Beysens [43], Maestre-Valero [15], Jürges [44], Watmuff [45], Kumar [46], Sharples [47], and Test [48].

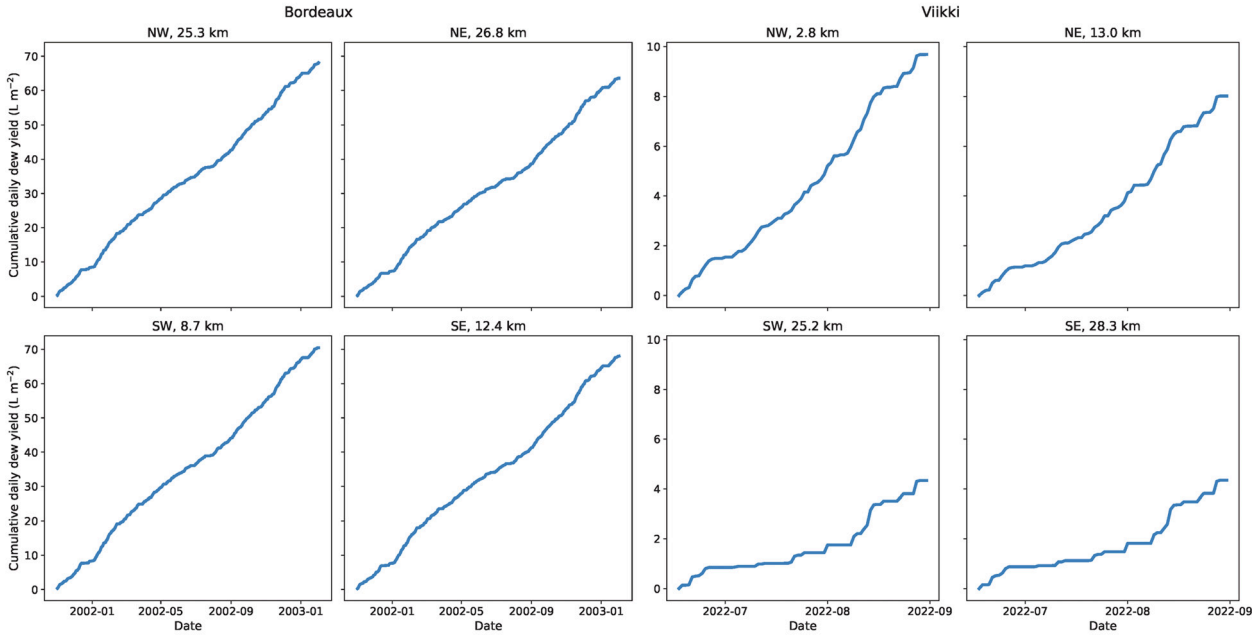


Figure A2. Sensitivity of cumulative simulated dew yield to ERA5 grid-cell selection for two representative sites, Bordeaux and Helsinki. Four neighboring grid cells around each study site were used. The results show moderate sensitivity at Bordeaux and substantially larger sensitivity at Helsinki, where neighboring grid cells differ more strongly in land–water representation.

References

1. Zheng, Z.; Hoogenboom, G.; Cai, H.; Wang, Z. Winter Wheat Production on the Guanzhong Plain of Northwest China under Projected Future Climate with SimCLIM. *Agric. Water Manag.* **2020**, *239*, 106233. [CrossRef]
2. Sun, D.; Kherazi, F.Z.; Shaikh, S.N. Elevation-Dependent Ecohydrological Decoupling and Basin-Scale Vulnerability: A 25-Year Assessment of Water–Vegetation Interactions in the Jinsha River Basin. *Ecohydrol. Hydrobiol.* **2026**, *26*, 100729. [CrossRef]
3. Kord, S.M.Z.; Tuure, J.; Räsänen, M.; Galambosi, S.; Alakukku, L. Geometry and Surface Manipulation Impact on Passive Dew and Rain Collection. *Agric. For. Meteorol.* **2024**, *356*, 110180. [CrossRef]
4. Kord, S.M.Z.; Tuure, J.; Räsänen, M.; Galambosi, S.; Alakukku, L. Automatic Wiping Effect on Passive Dew Collection. *Agric. For. Meteorol.* **2025**, *375*, 110891. [CrossRef]
5. Tuure, J.; Korpela, A.; Hautala, M.; Rautkoski, H.; Hakojärvi, M.; Mikkola, H.; Duplissy, J.; Pellikka, P.; Petäjä, T.; Kulmala, M.; et al. Comparing Plastic Foils for Dew Collection: Preparatory Laboratory-Scale Method and Field Experiment in Kenya. *Biosyst. Eng.* **2020**, *196*, 145–158. [CrossRef]
6. Muselli, M.; Beysens, D.; Marcillat, J.; Milimouk, I.; Nilsson, T.; Louche, A. Dew Water Collector for Potable Water in Ajaccio (Corsica Island, France). *Atmos. Res.* **2002**, *64*, 297–312. [CrossRef]
7. Beysens, D. *Dew Water*; River Publishers: Delft, The Netherlands, 2018; ISBN 978-87-93609-47-1.
8. Beysens, D. Estimating Dew Yield Worldwide from a Few Meteo Data. *Atmos. Res.* **2016**, *167*, 146–155. [CrossRef]
9. Berkowicz, S.M.; Beysens, D.; Milimouk, I.; Heusinkveld, B.G.; Muselli, M.; Wakshal, E.; Jacobs, A.F.G. Urban Dew Collection Under Semi-Arid Conditions: Jerusalem. In *Proceedings of the Third International Conference on Fog, Fog Collection and Dew*; ARC-ISCW: Pretoria, South Africa, 2004; p. E4.
10. Sharan, G.; Clus, O.; Singh, S.; Muselli, M.; Beysens, D. A Very Large Dew and Rain Ridge Collector in the Kutch Area (Gujarat, India). *J. Hydrol.* **2011**, *405*, 171–181. [CrossRef]
11. Sharan, G.; Beysens, D.; Milimouk-Melnytchouk, I. A Study of Dew Water Yields on Galvanized Iron Roofs in Kothara (North-West India). *J. Arid Environ.* **2007**, *69*, 259–269. [CrossRef]
12. Jacobs, A.F.G.; Heusinkveld, B.G.; Berkowicz, S.M. Passive Dew Collection in a Grassland Area, The Netherlands. *Atmos. Res.* **2008**, *87*, 377–385. [CrossRef]
13. Lekouch, I.; Muselli, M.; Kabbachi, B.; Ouazzani, J.; Melnytchouk-Milimouk, I.; Beysens, D. Dew, Fog, and Rain as Supplementary Sources of Water in South-Western Morocco. *Energy* **2011**, *36*, 2257–2265. [CrossRef]
14. Clus, O.; Ouazzani, J.; Muselli, M.; Nikolayev, V.S.; Sharan, G.; Beysens, D. Comparison of Various Radiation-Cooled Dew Condensers Using Computational Fluid Dynamics. *Desalination* **2009**, *249*, 707–712. [CrossRef]

15. Maestre-Valero, J.F.; Martínez-Alvarez, V.; Baille, A.; Martín-Górriz, B.; Gallego-Elvira, B. Comparative Analysis of Two Polyethylene Foil Materials for Dew Harvesting in a Semi-Arid Climate. *J. Hydrol.* **2011**, *410*, 84–91. [CrossRef]
16. Nilsson, T. Initial Experiments on Dew Collection in Sweden and Tanzania. *Sol. Energy Mater. Sol. Cells* **1996**, *40*, 23–32. [CrossRef]
17. Monteith, J.L. Dew. *Q. J. R. Meteorol. Soc.* **1957**, *83*, 322–341. [CrossRef]
18. Monteith, J.L.; Unsworth, M.H. *Principles of Environmental Physics: Plants, Animals, and the Atmosphere*, 4th ed.; Elsevier: Amsterdam, The Netherlands; Academic Press: Boston, MA, USA, 2013; ISBN 978-0-12-386910-4.
19. Beysens, D.; Muselli, M.; Milimouk, I.; Ohayon, C.; Berkowicz, S.; Soyeux, E.; Mileta, M.; Ortega, P. Application of Passive Radiative Cooling for Dew Condensation. *Energy* **2006**, *31*, 2303–2315. [CrossRef]
20. Beysens, D.; Milimouk, I.; Nikolayev, V.; Muselli, M.; Marcillat, J. Using Radiative Cooling to Condense Atmospheric Vapor: A Study to Improve Water Yield. *J. Hydrol.* **2003**, *276*, 1–11. [CrossRef]
21. Nikolayev, V.S.; Beysens, D.; Gioda, A.; Milimouka, I.; Katiushin, E.; Morel, J.-P. Water Recovery from Dew. *J. Hydrol.* **1996**, *182*, 19–35. [CrossRef]
22. Anand, S.; Rykaczewski, K.; Subramanyam, S.B.; Beysens, D.; Varanasi, K.K. How Droplets Nucleate and Grow on Liquids and Liquid Impregnated Surfaces. *Soft Matter* **2015**, *11*, 69–80. [CrossRef] [PubMed]
23. Pedro, M.J.; Gillespie, T.J. Estimating Dew Duration. I. Utilizing Micrometeorological Data. *Agric. Meteorol.* **1981**, *25*, 283–296. [CrossRef]
24. Tomaszkiewicz, M.; Abou Najm, M.; Beysens, D.; Alameddine, I.; El-Fadel, M. Dew as a Sustainable Non-Conventional Water Resource: A Critical Review. *Environ. Rev.* **2015**, *23*, 425–442. [CrossRef]
25. Richards, K. Adaptation of a Leaf Wetness Model to Estimate Dewfall Amount on a Roof Surface. *Agric. For. Meteorol.* **2009**, *149*, 1377–1383. [CrossRef]
26. Beysens, D. Corrigendum to "Estimating Dew Yield Worldwide from a Few Meteo Data" [Atmospheric Research 167 (2016) 146–155]. *Atmos. Res.* **2022**, *267*, 105911. [CrossRef]
27. Atashi, N.; Tuure, J.; Alakukku, L.; Rahimi, D.; Pellikka, P.; Zaidan, M.A.; Vuollekoski, H.; Räsänen, M.; Kulmala, M.; Vesala, T.; et al. An Attempt to Utilize a Regional Dew Formation Model in Kenya. *Water* **2021**, *13*, 1261. [CrossRef]
28. Vuollekoski, H.; Vogt, M.; Sinclair, V.A.; Duplissy, J.; Järvinen, H.; Kyrö, E.-M.; Makkonen, R.; Petäjä, T.; Prisle, N.L.; Räisänen, P.; et al. Estimates of Global Dew Collection Potential on Artificial Surfaces. *Hydrol. Earth Syst. Sci.* **2015**, *19*, 601–613. [CrossRef]
29. Atashi, N.; Rahimi, D.; Goortani, B.M.; Duplissy, J.; Vuollekoski, H.; Kulmala, M.; Vesala, T.; Hussein, T. Spatial and Temporal Investigation of Dew Potential Based on Long-Term Model Simulations in Iran. *Water* **2019**, *11*, 2463. [CrossRef]
30. Atashi, N.; Rahimi, D.; Sinclair, V.A.; Zaidan, M.A.; Rusanen, A.; Vuollekoski, H.; Kulmala, M.; Vesala, T.; Hussein, T. Delineation of Dew Formation Zones in Iran Using Long-Term Model Simulations and Cluster Analysis. *Hydrol. Earth Syst. Sci.* **2021**, *25*, 4719–4740. [CrossRef]
31. Jacob, D.; Teichmann, C.; Sobolowski, S.; Katragkou, E.; Anders, I.; Belda, M.; Benestad, R.; Boberg, F.; Buonomo, E.; Cardoso, R.M.; et al. Regional Climate Downscaling over Europe: Perspectives from the EURO-CORDEX Community. *Reg. Environ. Change* **2020**, *20*, 51. [CrossRef]
32. Jacob, D.; Petersen, J.; Eggert, B.; Alias, A.; Christensen, O.B.; Bouwer, L.M.; Braun, A.; Colette, A.; Déqué, M.; Georgievski, G.; et al. EURO-CORDEX: New High-Resolution Climate Change Projections for European Impact Research. *Reg. Environ. Change* **2014**, *14*, 563–578. Erratum in *Reg. Environ. Change* **2014**, *14*, 579–581. https://doi.org/10.1007/s10113-014-0587-y. [CrossRef]
33. Gutowski, W.J., Jr.; Giorgi, F.; Timbal, B.; Frigon, A.; Jacob, D.; Kang, H.-S.; Raghavan, K.; Lee, B.; Lennard, C.; Nikulin, G.; et al. WCRP COordinated Regional Downscaling EXperiment (CORDEX): A Diagnostic MIP for CMIP6. *Geosci. Model Dev.* **2016**, *9*, 4087–4095. [CrossRef]
34. Aphalo, P.J. *High Frequency Weather Data for Viikki, Helsinki, Finland*; Open Science Framework: Washington, DC, USA, 2021. [CrossRef]
35. Lawrence, M.G. The Relationship between Relative Humidity and the Dewpoint Temperature in Moist Air: A Simple Conversion and Applications. *Bull. Am. Meteorol. Soc.* **2005**, *86*, 225–234. [CrossRef]
36. Alduchov, O.A.; Eskridge, R.E. Improved Magnus Form Approximation of Saturation Vapor Pressure. *J. Appl. Meteorol. Climatol.* **1996**, *35*, 601–609. [CrossRef] [PubMed]
37. Beysens, D.; Lefavrais, S.; Muselli, M.; Rébillout, P.; Royon, L. A Standard for Dew Measurement. *J. Hydrol.* **2025**, *661*, 133527. [CrossRef]
38. Hersbach, H.; Bell, B.; Berrisford, P.; Hirahara, S.; Horányi, A.; Muñoz-Sabater, J.; Nicolas, J.; Peubey, C.; Radu, R.; Schepers, D.; et al. The ERA5 Global Reanalysis. *Q. J. R. Meteorol. Soc.* **2020**, *146*, 1999–2049. [CrossRef]
39. Soci, C.; Hersbach, H.; Simmons, A.; Poli, P.; Bell, B.; Berrisford, P.; Horányi, A.; Muñoz-Sabater, J.; Nicolas, J.; Radu, R.; et al. The ERA5 Global Reanalysis from 1940 to 2022. *Q. J. R. Meteorol. Soc.* **2024**, *150*, 4014–4048. [CrossRef]
40. Tian, C.; Jiao, W.; Beysens, D.; Farai Kaseke, K.; Medici, M.-G.; Li, F.; Wang, L. Investigating the Role of Evaporation in Dew Formation under Different Climates Using 17O-Excess. *J. Hydrol.* **2021**, *592*, 125847. [CrossRef]

41. Giorgi, F.; Jones, C.; Asrar, G.R. Addressing Climate Information Needs at the Regional Level the CORDEX Framework. *WMO Bull.* **2009**, *58*, 175–183.
42. Yavaşlı, D.D.; Erlat, E. Tropical Nights in the Mediterranean: A Spatiotemporal Analysis of Trends from 1950 to 2022. *Int. J. Climatol.* **2024**, *44*, 1472–1488. [CrossRef]
43. Beysens, D.; Muselli, M.; Nikolayev, V.; Narhe, R.; Milimouk, I. Measurement and Modelling of Dew in Island, Coastal and Alpine Areas. *Atmos. Res.* **2005**, *73*, 1–22. [CrossRef]
44. Jürges, W. *Der Wärmeübergang an Einer Ebenen Wand; Beihefte zum Gesundheits-Ingenieur*; Druck und Verlag von R. Oldenbourg: München und Berlin, Germany, 1924.
45. Watmuff, J.H.; Charters, W.W.S.; Proctor, D. Solar and Wind Induced External Coefficients Solar Collectors. *Rev. Int. Heliotech.* **1977**, *2*, 56. Available online: https://www.scirp.org/reference/referencespapers?referenceid=1048678&utm_source=chatgpt.com (accessed on 23 June 2026).
46. Kumar, S.; Sharma, V.B.; Kandpal, T.C.; Mullick, S.C. Wind Induced Heat Losses from Outer Cover of Solar Collectors. *Renew. Energy* **1997**, *10*, 613–616. [CrossRef]
47. Sharples, S.; Charlesworth, P.S. Full-Scale Measurements of Wind-Induced Convective Heat Transfer from a Roof-Mounted Flat Plate Solar Collector. *Sol. Energy* **1998**, *62*, 69–77. [CrossRef]
48. Test, F.L.; Lessmann, R.C.; Johary, A. Heat Transfer During Wind Flow over Rectangular Bodies in the Natural Environment. *J. Heat Transf.* **1981**, *103*, 262–267. [CrossRef]

Disclaimer/Publisher's Note: The statements, opinions and data contained in all publications are solely those of the individual author(s) and contributor(s) and not of MDPI and/or the editor(s). MDPI and/or the editor(s) disclaim responsibility for any injury to people or property resulting from any ideas, methods, instructions or products referred to in the content.